



Mini-Review: Mixed Ionic–Electronic Charge Carrier Localization and Transport in Hybrid Organic–Inorganic Nanomaterials

Mariano Romero*, Dominique Mombrú, Fernando Pignanelli, Ricardo Faccio* and Alvaro W. Mombrú*

Centro NanoMat & Área Física, Departamento de Experimentación y Teoría de la Estructura de la Materia y sus Aplicaciones - DETEMA, Facultad de Química, Universidad de la República, Montevideo, Uruguay

OPEN ACCESS

Edited by:

Rengaraj Selvaraj,
Sultan Qaboos University, Oman

Reviewed by:

Xiaopeng Han,
Tianjin University, China
Guillermo Javier Copello,
Consejo Nacional de Investigaciones
Científicas y Técnicas
(CONICET), Argentina

*Correspondence:

Mariano Romero
mromero@fq.edu.uy
Ricardo Faccio
rfaccio@fq.edu.uy
Alvaro W. Mombrú
amombrú@fq.edu.uy

Specialty section:

This article was submitted to
Nanoscience,
a section of the journal
Frontiers in Chemistry

Received: 16 April 2020

Accepted: 26 May 2020

Published: 14 July 2020

Citation:

Romero M, Mombrú D, Pignanelli F,
Faccio R and Mombrú AW (2020)
Mini-Review: Mixed Ionic–Electronic
Charge Carrier Localization and
Transport in Hybrid Organic–Inorganic
Nanomaterials. *Front. Chem.* 8:537.
doi: 10.3389/fchem.2020.00537

In this mini-review, a comprehensive discussion on the state of the art of hybrid organic–inorganic mixed ionic–electronic conductors (*hOI*-MIECs) is given, focusing on conducting polymer nanocomposites comprising inorganic nanoparticles ranging from ceramic-in-polymer to polymer-in-ceramic concentration regimes. First, a brief discussion on fundamental aspects of mixed ionic–electronic transport phenomena considering the charge carrier transport at bulk regions together with the effect of the organic–inorganic interphase of hybrid nanocomposites is presented. We also make a recount of updated instrumentation techniques to characterize structure, microstructure, chemical composition, and mixed ionic–electronic transport with special focus on those relevant for *hOI*-MIECs. Raman imaging and impedance spectroscopy instrumentation techniques are particularly discussed as relatively simple and versatile tools to study the charge carrier localization and transport at different regions of *hOI*-MIECs including both bulk and interphase regions to shed some light on the mixed ionic–electronic transport mechanism. In addition, we will also refer to different device assembly configurations and *in situ/operando* measurements experiments to analyze mixed ionic–electronic conduction phenomena for different specific applications. Finally, we will also review the broad range of promising applications of *hOI*-MIECs, mainly in the field of energy storage and conversion, but also in the emerging field of electronics and bioelectronics.

Keywords: hybrid organic–inorganic composites, nanomaterials, mixed ionic–electronic conducting materials, semiconductor, Raman micro spectroscopy, impedance spectroscopy

INTRODUCTION

In the last decades, mixed ionic–electronic conductors (MIECs) have been widely studied for energy storage and energy conversion materials, separation membranes, and catalysts (Shao and Haile, 2004; Maier, 2005; Wachsmann and Lee, 2011; Aoki et al., 2014). Both ionic (σ_i) or electronic (σ_e) conduction obey separately and analogously to the following equation:

$$\sigma = qN\mu \quad (1)$$

where q is the charge, N is the number, and μ is the mobility of the charge carrier, the latter being proportional to diffusivity (D). In the particular case of inorganic MIECs, some well-known

examples are semiconducting compounds such as Ag_2X (with $\text{X} = \text{S}, \text{Se}, \text{or Te}$) as mixed silver ion (Ag^+) and electronic conducting materials (Yokota, 1961; Miyatani, 1973; Riess, 2003) and A-doped MO_{2-8} (typically $M = \text{Ce}$ or Zr , and A being different dopants) as mixed oxygen ion (O^{2-}) and electronic transport materials (Goodenough, 2000; Balaguer et al., 2011; Lin et al., 2015). However, one of the most relevant inorganic MIEC materials gaining special attention in the recent years are $\text{A}_x\text{M}_2\text{O}_4$ (with $M = \text{Ni}, \text{Co}, \text{and/or Mn}$ and $A = \text{Li}$ or Na) due to their excellent performance, particularly as cathode materials for lithium (Li^+) and sodium (Na^+) ion batteries (Doeff et al., 1993; Barker et al., 1996; Saïdi et al., 1996; Thackeray, 1997; Dokko et al., 2001; Lu and Dahn, 2001; Cao and Prakash, 2002; Levasseur et al., 2002; Sauvage et al., 2007; Berthelot et al., 2010; Tevar and Whitacre, 2010). For instance, typical electronic conductivities (σ_e) and lithium-ion diffusivities (D_i) for $\text{Li}_x\text{M}_2\text{O}_4$ cathode materials are $\sigma_e \sim 10^{-6}$ - 10^{-1} S cm^{-1} and $D_i \sim 10^{-11}$ - 10^{-8} cm^2s^{-1} , respectively, depending strongly on the transition metal (M), lithiation degree (x), and crystallinity (Park et al., 2010). In the particular case of semiconducting inorganic nanomaterials, both ionic and electronic transport present lower charge carrier resistance at the crystalline bulk regions but are drastically compromised by the poor charge carrier conducting nature of grain boundaries (Park et al., 2010). In the last decades, the addition of conducting coating materials and secondary phases such as mixed ionic–electronic conducting organic materials (e.g., conducting polymers), working as linkers between inorganic nanomaterials, has attracted a lot of attention (Judeinstein and Sanchez, 1996; Gómez-Romero and Lira-Cantú, 1997; Guizard et al., 2001; Le Bideau et al., 2011). It is well-accepted that electronic conducting organic polymers, usually called conjugated polymers, are semiconductors in nature and that the most popular cases such as poly(pyrrrole) (Ppy) (Della Santa et al., 1997), poly(aniline) (PANI) (Zhang K. et al., 2012a; Chatterjee et al., 2013; Zhang Q. et al., 2013a; Roussel et al., 2015), poly(ethylenedioxythiophene) (PEDOT) (Crispin et al., 2006; Udo et al., 2009; Takano et al., 2012; Kim et al., 2013; Mengistie et al., 2013, 2015; Lee et al., 2014; Kumar et al., 2016; Zia Ullah et al., 2016), and poly(3-hexylthiophene) (P3HT) (Zhang Q. et al., 2012; Pingel and Neher, 2013; Gludell et al., 2015; Jacobs et al., 2016; Qu et al., 2016; Jung et al., 2017; Wang W. et al., 2017; Lim et al., 2018) generally exhibit an electronic donor behavior. In this case, the most common procedure to enhance the electronic conduction, where charge carriers will be mostly holes rather than electrons, is by doping these polymers with electronic acceptor species (p-type doping) such as halide and sulfonate salts, yielding a decrease in the electronic band gap and an increase of the electronic conductivity up to $\sigma_e \sim 10^{-1}$ - 10^3 S cm^{-1} values (Della Santa et al., 1997; Crispin et al., 2006; Udo et al., 2009; Takano et al., 2012; Zhang K. et al., 2012; Zhang Q. et al., 2012, 2013; Chatterjee et al., 2013; Kim et al., 2013; Mengistie et al., 2013, 2015; Pingel and Neher, 2013; Lee et al., 2014; Gludell et al., 2015; Roussel et al., 2015; Jacobs et al., 2016; Kumar et al., 2016; Qu et al., 2016; Zia Ullah et al., 2016; Jung et al., 2017; Wang W. et al., 2017; Lim et al., 2018). The mere presence of the dopant, typically halide, or sulfonate salts with relatively high degree of

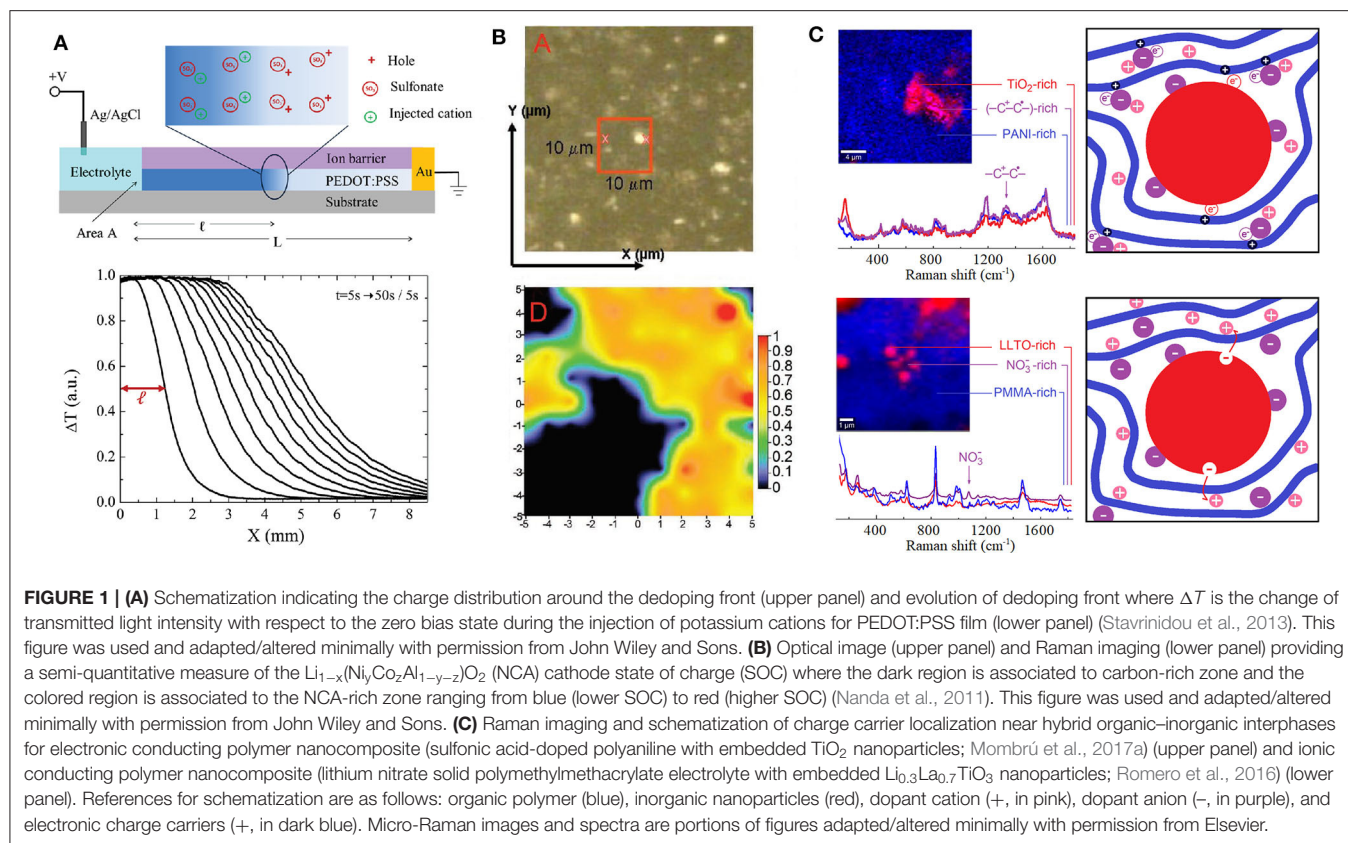
dissociation, will trigger a non-negligible ionic conduction in addition to the electronic transport (Riess, 2000). It is important to mention that there are other “non-dissociable” excellent dopants such as the case of tetracyanoquinodimethane (TCNQ) in all of its fluorinated forms, but as it does not provide highly mobile ionic carriers, it will not be considered in this review. It was long observed that protons (H^+), lithium (Li^+), sodium (Na^+), or potassium (K^+) cations yielded a considerable ionic contribution to the total mixed ionic–electronic transport of conjugated polymers (Nigrey et al., 1978; Aldebert et al., 1986; Barthet and Guglielmi, 1995; Watanabe, 1996). The voluminous dopant anions are generally more fixed to the polymer chain, allowing the electronic exchange process (doping) to take place but contributing in a lesser extent to the ionic conductivity except for a few particular cases (Cheng et al., 2005). Pursuing an increase in the ionic conduction of MIECs, blending and co-polymerization (including functionalization of side chains) of electronic conducting polymers with good ionic conducting polymers [e.g., poly(ethylene oxide) (PEO)], has shown enhancement of ionic conductivities up to $\sigma_i \sim 10^{-5}$ - 10^{-4} S cm^{-1} (Li and Khan, 1991; Barthet et al., 1997; Ghosh and Inganäs, 2000; Zhang et al., 2002; Patel et al., 2012; Ju et al., 2014; Kang et al., 2014; Dong et al., 2019; Sengwa and Dhatwarwal, 2020). Another strategy includes the simultaneous doping and blending of electronic conducting polymers with polymeric dopants, particularly observed for protons and lithium-ion charge carriers (Murthy and Manthiram, 2011; Fu and Manthiram, 2012; Liu et al., 2012). However, it is important to remark that the inclusion of electronic-insulating polymers inevitably leads to the declining of the electronic conductivity ($\sigma_e \sim 10^{-5}$ S cm^{-1} , i.e., several orders of magnitude less than the isolated conducting polymer in its doped form), and thus, electronic-conducting polymer/ionic-conducting polymer/dopant concentrations need to be rationally balanced (Li and Khan, 1991; Barthet et al., 1997; Ghosh and Inganäs, 2000; Zhang et al., 2002; Murthy and Manthiram, 2011; Fu and Manthiram, 2012; Liu et al., 2012; Patel et al., 2012; Ju et al., 2014; Kang et al., 2014; Dong et al., 2019; Sengwa and Dhatwarwal, 2020). Recent comprehensive reviews discussing different types of organic MIEC classes, with particular focus on taxonomy and electronic–ionic interactions, are given by Paulsen et al. (2020), and a thorough discussion of morphologic effects on organic polymeric MIEC is given by Onorato and Luscombe (2019). On the other hand, it is well-known that the addition of semiconducting ceramic nanoparticles, even with negligible intrinsic electronic (or ionic) transport ability, can also yield an enhancement of the electronic (or ionic) conduction in conducting polymer nanocomposites. For instance, the presence of inorganic nanoparticles, particularly transition metal oxides, has yielded a notorious increment of electronic conductivity for electronic–conductor polymer nanocomposites in both ceramic-in-polymer (Mombrú et al., 2017a,b; Mombrú et al., 2019) and polymer-in-ceramic concentration regimes (Huguenin et al., 2004; Wang et al., 2010; Mombrú et al., 2017a). In analogy, the presence of inorganic nanoparticles resulted in an enhancement on the ionic conductivity for ionic conductor polymer nanocomposites (Kloster et al., 1996; Scrosati et al., 2000; Shin and Passerini, 2004). The presence

of secondary phases or inorganic nanofillers induces slight structural modifications, altering the degree of order of the conducting polymer chains that could explain the enhancement of the conductivity, without considering direct mediation of charge carriers through the nanoparticle interphase. Although it is accepted that the electronic conduction in polymer nanocomposites is usually related to higher crystallinity (or higher degree of order), the enhancement of the ionic conduction is mostly associated to lower crystallinity (or lower degree of order), but the latter case is still under recent debate (Onorato and Luscombe, 2019). Furthermore, in the case of ceramic nanoparticles' interaction with conducting polymers, the presence of an interphase between both organic and inorganic materials adds a particular complexity to the system and can eventually lead to important consequences in both ionic and electronic transport properties. Leaving out drastic effects such as voids, poor contact, or the presence of decomposition phases due to eventual chemical reactions, it is extremely difficult to obtain well-defined interphases between such different materials. For instance, the presence of defects, mainly in the inorganic nanoparticle boundaries, can lead to the presence of charge localization at the interphase and the presence of different crystallographic surfaces of the inorganic nanoparticle at the interphase can exhibit different electronic interactions with the polymer phase. Up to now, to the best of our knowledge, there are only a few reviews of MIEC materials with particular focus on their applications such as energy (Sengodu and Deshmukh, 2015), bioelectronics (Han S. et al., 2019), and sensing (Inal et al., 2018), but no further insights into *hOI*-MIECs. In this mini-review, charge carrier localization and transport at different regions of *hOI*-MIECs including both bulk and interphase regions is revised, focusing on the use of some powerful and versatile instrumental techniques.

CHARGE CARRIER LOCALIZATION

There are a lot of instrumentation techniques that can provide particularly rich information about structural features of *hOI*-MIECs such as Nuclear Magnetic Resonance (NMR), X-ray diffraction (XRD), and wide-/small-angle X-ray scattering (WAXS/SAXS) in both transmission or grazing incidence configurations (Sanjeeva Murthy, 2016). However, it is important to remark that X-ray scattering techniques are relatively accessible but generally give indirect information about charge carrier localization and on the other hand, although NMR could be very powerful to monitor charge carrier's location, it is particularly less versatile than other optical spectroscopies techniques. For instance, a relatively simple and powerful method to monitor not only charge localization but also drift mobility in organic MIECs is the "moving front" experiment, which is based on visible light transmission monitoring through an electrochromic film as it is dedoped due to lateral injection of H^+ , Na^+ , or K^+ ions from a planar junction with an electrolyte, as shown in **Figure 1A** (Stavriniidou et al., 2013; Rivnay et al., 2016). Nonetheless, one of the most popular but no less powerful and versatile technique to study structural features of *hOI*-MIECs

is vibrational spectroscopy. Raman spectroscopy is particularly interesting for inorganic materials characterization as it does not exclude highly amorphous systems in comparison with XRD and provides accessibility to vibrational modes with lower wavenumbers (typically $\nu_{\min} \sim 80\text{--}100\text{ cm}^{-1}$) in comparison to infrared spectroscopy (typically $\nu_{\min} \sim 200\text{--}400\text{ cm}^{-1}$). Raman spectroscopy also has the remarkable advantage of needing little sample preparation, allowing the study of materials in its native conditions, as well as permitting collection of *in situ* and *in operando* measurements. For instance, *in situ/operando* Raman spectroscopy has allowed the study of the state of charge of $(Li, Na, K)_xM_2O_4$ electrodes by monitoring the broadening and shifting of Raman peaks when lowering Li, Na, or K content from nominal $X = 1$ (full charged cathode), particularly associated to the loss of ions from the interlayer of the MO_2 layered structure (Dokko et al., 2003; Nanda et al., 2011; Nishi et al., 2013; Chen et al., 2015; Flores et al., 2018). An example on the use of Raman imaging to monitor the state of charge for a $Li_{1-x}(Ni_yCo_zAl_{1-y-z})O_2$ cathode is shown and described briefly in **Figure 1B** (Nanda et al., 2011). In addition, the use of micro-Raman imaging technique is highly powerful to study simultaneously both compositional and microstructural features, especially for hybrid inorganic-organic materials, as the characteristic Raman signals for inorganic and organic compounds generally lie well-separated at lower ($\nu < 800\text{ cm}^{-1}$) and higher ($\nu > 800\text{ cm}^{-1}$) wavenumbers, respectively (Romero et al., 2016; Mombrú et al., 2017a,b,c; Pignanelli et al., 2018, 2019a,b). Furthermore, although Raman spectroscopy is quite sensitive to diluted effects such as doping processes of inorganic materials, it is on the other hand, extremely sensitive to doping effects of organic materials such as conducting polymers (Furukawa, 1996). Briefly, the doping process of conducting polymers yields to drastic modifications of the Raman signature in relation to the charge carrier formation, typically in the form of positive polarons ($-C^+-C^{\bullet-}$) or bipolarons ($-C^+-C^{+}-$), particularly altering both Raman frequency and activity of vibrational modes associated to carbon-to-carbon ($C=C$) molecular bonds in conjugated polymers (Furukawa, 1996; Kumar et al., 2012; Yamamoto and Furukawa, 2015; Francis et al., 2017; Mombrú et al., 2018; Nightingale et al., 2018). For instance, micro-Raman imaging has evidenced the presence of these types of charge carriers particularly localized near the interphase with inorganic nanoparticles; [e.g., MX_2 with M being different transition metals and $X = O$ (for oxides) or S (for sulfides) (Mombrú et al., 2017a,b,c; Mombrú et al., 2019)]. The increment of conducting polymer electronic charge carriers near the interphase could be discussed in view of at least two eventual scenarios: (one or *passive*) the dopant stabilizes at the interphase due to strong polar or coulombic interactions with nanoparticles surface, or/and (two or *active*) the nanoparticles are also good electronic acceptors, producing in both cases an enhancement on the doping of nearby polymer chains, as schematized in **Figure 1C** (upper panel). On the other hand, micro-Raman imaging has also been useful to evidence the enhancement of ionic-pair dissociation occurring near the interphase with inorganic nanoparticles, in agreement with the increment of ionic conductivity (Romero et al., 2016; Pignanelli et al., 2018,



Pignaneli et al., 2019a). Analogously, two different scenarios could be discussed for ionic charge carriers: (one or *passive*) the counter-ion (in analogy to the dopant anion) stabilizes at the interphase due to strong polar or coulombic interactions with nanoparticles surface yielding an enhancement on the ionic-pair dissociation, or/and (two or *active*) the nanoparticles may also possess mobile ionic carriers at the surface (e.g., active filler) that can be injected into the polymer, as schematized in **Figure 1C** (lower panel). Whatever the case, the previous micro-Raman imaging studies revealed that the interphase of organic-inorganic nanocomposites, to a greater or lesser extent, always play an important role in the charge carrier transport mechanism.

CHARGE CARRIER CONDUCTION

There are several electrochemical methodologies to study the charge carrier conduction in MIECs, but one of the most powerful techniques to access both electronic and ionic transport simultaneously is impedance spectroscopy (Jamnik and Maier, 1999; Vorotyntsev et al., 1999; Huggins, 2002; Atkinson et al., 2004; Lee et al., 2009). Briefly, the impedance response as a function of the frequency (typically 10^{-3} - 10^6 Hz) of an oscillating voltage (typically 10–100 mV amplitude) can provide information about different charge carriers with different relaxation times (τ) depending on their q/m ratio; [i.e., the higher

the q/m ratio, the lower τ and the higher associated frequencies ($f = 2\pi/\tau$)]. In this case, the Nyquist representation of impedance (imaginary impedance vs. real impedance, $-Z''$ vs. Z') for a single electronic semiconductor in a continuous medium will show a single semicircle arc. The semicircle arc associated to the electronic carrier transport can be typically modeled using the parallel combination of a resistor (R_e) and a capacitor (C_e). In analogy, but with probably higher associated τ (lower f), a single ionic conductor in a continuous medium will also show a similar single semicircle arc associated to the ionic carrier transport that can also be modeled using the parallel combination of a resistor (R_i) and a capacitor (C_i), whose associated charge carrier pathway is represented with a straight line in **Figure 2A**. If an additional pathway is mediating the electronic (or ionic) transport (e.g., the presence of grain boundaries or depletion regions in less crystalline solids), a second $R_e C_e'$ (or $R_i C_i'$) parallel combination connected in series with the previous one is usually necessary to fit the total impedance response, whose associated charge carrier pathway is represented with a zig-zag line in **Figure 2A**. For simplicity, from now on, we will only consider the charge carrier transport of ionic and electronic conductor samples assembled in a symmetric cell configuration using ideal metallic ion-blocking electrodes. This means that only electronic carriers will be short-circuited and ionic species will be blocked at the interphase with the ion-blocking metallic electrodes but the opposite will apply in the case of using electronic-blocking electrodes. In the case of using metallic ion-blocking electrodes, in addition to

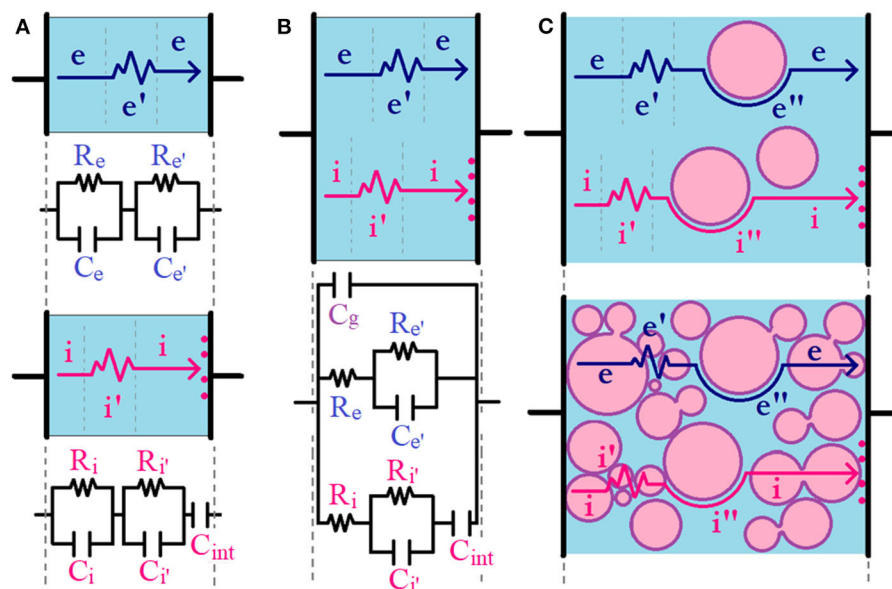


FIGURE 2 | Circuit model schematization for (A) separated electronic and ionic transport in a single phase, (B) mixed ionic–electronic transport in a single phase, and (C) mixed ionic–electronic transport in *hOI*-MIECs ranging from ceramic-in-polymer (upper panel) to polymer-in-ceramic (lower panel). Electronic and ionic hypothetical pathways are shown with dark blue and pink arrows. The zigzag part of the arrows indicates the presence of eventual grain boundaries or depleted regions [with associated ionic (i') or electronic (e') contributions] and the curved part of the arrows indicates the presence of eventual transport pathway mediated through organic–inorganic interfacial regions [with associated ionic (i'') and electronic (e'') contributions].

the semicircle arc observed at higher frequencies, the Nyquist plots of single ionic conductors will also show an additional capacitive tail at low frequencies (C_{int}), which is associated to the polarization of blocked ions at the sample/electrode interphase, as shown in **Figure 2A**. If now we consider the simplest case of a MIEC material, the bi-continuous ionic and electronic channels can be strategically represented by the parallel combination of ionic and electronic resistances (R_i and R_e , respectively) together with a global geometrical capacitance (C_g), with the associated pathway represented by a straight line in **Figure 2B**. It is important to remark that the C_{int} element only appears connected in series with the ionic resistance as we are working with ideal ion-blocking electrodes, but the opposite will occur (i.e., an analogous C_{int} element will only appear connected in series with the electronic resistance) if we are working with electronic-blocking electrodes. The origin of this circuit model simplification is described thoroughly by Jamnik and Maier and is only applicable for macroscopically thick samples considering ideal selectively ion-blocking electrodes and chemical capacitance much larger than the interfacial capacitance of the blocked carriers (Jamnik and Maier, 1999; Lee et al., 2009). In the case that any of the electronic or ionic transport is mediated by the presence of a secondary pathway in a MIEC, generally associated to grain boundaries or depleted regions, as we discuss before, a second $R_{e'}C_{e'}$ (or $R_{i'}C_{i'}$) parallel combination connected in series with R_e (or R_i), respectively, could be useful to fit the total impedance response, with associated pathway represented by a zig-zag line in **Figure 2B** (Huggins, 2002). In the recent literature, both the inclusion and exclusion of

this second $R_{e'}C_{e'}$ (or $R_{i'}C_{i'}$) parallel combination in biphasic polymeric MIECs have been observed, depending mainly on the electronic- and ionic-conducting phase concentration or microstructural differences (Patel et al., 2012; Renna et al., 2017). In the particular case of *hOI*-MIECs, the second contribution (and probably a third contribution) to ionic or electronic transport could be present due to the mere existence of the organic–inorganic interphase, as shown in **Figure 2C**. However, even for a simplified experiment configuration, (e.g., using symmetric ion-blocking electrodes), it is important to rationalize the number of elements in a given circuit model to avoid over-parametrization. For instance, in the extreme case of *hOI*-MIECs based on a continuous organic semiconductor, [e.g., conducting polymer with diluted inorganic nanoparticle additives (ceramic-in-polymer)], both electronic and ionic carriers will be mainly transported through the organic matrix. For instance, $R_{e'}C_{e'}$ and $R_{i'}C_{i'}$ elements could be eventually excluded from the circuit model in the presence of homogeneous (full crystalline or amorphous) polymeric phase. However, in consonance with the non-homogeneous localization of charge carriers discussed in the previous section, the presence of an organic–inorganic interphase can eventually activate another electronic or/and ionic pathway mediated through the interphase that could be passive or active (Irvine et al., 1990). For instance, solid polymer electrolytes with active inorganic nanofillers are the typical case of organic–inorganic interphase-mediated ionic transport (Zheng et al., 2016; Yang et al., 2017; Pignanelli et al., 2019a), and a similar behavior will be observed for the electronic counterpart, if there are electronic interactions at the organic–inorganic interphase

(Chen et al., 2010; Nowy et al., 2010; Cai et al., 2012; Mombrú et al., 2017b). This effect, whose associated charge carrier pathway is represented by a curved line in **Figure 2C**, can also be eventually modeled with $R_{e''}C_{e''}$ (or $R_{i''}C_{i''}$) elements connected in series with the electronic (or ionic) part of the mixed ionic–electronic circuit, in analogy to R_eC_e (or R_iC_i), respectively. However, as mentioned earlier in the previous section, even when the inorganic nanoparticles are passive or non-interacting in nature with charge carriers, the concentration of both electronic or ionic charge carriers at the vicinities of the organic–inorganic interphase could also be activating a second pathway to the charge carrier transport. Nonetheless, in the case of passive interphases, this effect could be rather weak and both charge carrier transport pathways are expected to be mainly through the organic phase without interphase mediation; thus, only a global contribution to the charge carrier transport is usually observed and additional $R_{e''}C_{e''}$ (or $R_{i''}C_{i''}$) elements are not necessary to fit the global impedance response. In the other extreme case, [i.e., *hOI*-MIECs based on inorganic semiconductor nanoparticles with diluted organic polymeric additives (polymer-in-ceramic)], both electronic and ionic carriers are mainly transported through the inorganic matrix. In this case, due to the inevitable presence of grain boundaries in inorganic semiconductor nanoparticles, R_eC_e (or R_iC_i) elements should always be considered, as this contribution practically governs the global electronic (or ionic) transport. In this case, the polymeric additions usually act as fillers of empty spaces between nanoparticles, resulting in an enhancement of the electronic (or ionic) conductivity, and this is usually evaluated directly on R_eC_e (or R_iC_i) elements. However, in the case of simultaneous presence of particle-to-particle and particle–polymer–particle interphases, there will be at least two different pathways to electronic (or ionic) transport and additional $R_{e''}C_{e''}$ (or $R_{i''}C_{i''}$) elements could be necessary to fit the polymer-mediated transport contribution, as depicted in **Figure 2C**.

APPLICATIONS

The successful synergistic properties between organic and inorganic MIECs have yielded excellent performances, especially in the field of energy storage and particularly for lithium- and sodium-ion battery electrode materials (Sengodu and Deshmukh, 2015). In this sense, active cathode or anode materials embedded in polymeric hosts not only increase the mixed ionic–electronic conduction but also act as a sort of protection to the decomposition of active materials (Sengodu and Deshmukh, 2015). For instance, in the case of lithium-ion battery cathode materials: hybrid P3HT-co-PEO/LiFePO₄ has improved the delivery of both ionic and electronic charge to active centers (Javier et al., 2011); Ppy/LiFePO₄ with different hierarchical structures promoted both electronic and ionic transport (Fedorkova et al., 2010; Shi et al., 2017); PEDOT/LiFePO₄ offers excellent discharge capacity (Vadivel Murugan et al., 2008); Ppy/ α -LiFeO₂ has improved the reversible capacity and cycling stability (Zhang et al., 2013); PPy/MoO₃, PPy/V₂O₅, PPy/LiCoO₂, and PPy/LiV₃O₈ yielded a reduction of charge

transfer resistance of the Li⁺ ion intercalation/deintercalation process (Wang et al., 2010; Tian et al., 2011; Tang et al., 2012a,b; Liu et al., 2013); and PEDOT-co-PEG/LiNi_{0.6}Co_{0.2}Mn_{0.2}O₂ showed high discharge capacity and enhanced transport of Li⁺ ions as well as electrons (Ju et al., 2014). Furthermore, in the case of lithium-ion anode materials, only to mention some examples, hybrid Ppy/SnO₂ yielded a more controlled Li⁺ diffusion (Yuan et al., 2007; Cui et al., 2011) and hybrid PANI-graphene/TiO₂ yielded fast charge-to-discharge rate and high enhanced cycling performance (Zhang F. et al., 2012). In the case of sodium-ion battery cathode materials, inorganic Na_xMO₂ oxides, NaMPO₄ phosphates, and Na[M'(CN)₆] hexacyanometalates (commonly known as Prussian blue analogs) have been tested (Xiang et al., 2015; Liu et al., 2020), and to a lesser extent, some organic MIEC polymers such as the case of Ppy (Zhou et al., 2012; Zhou et al., 2013; Zhu et al., 2013). However, in recent literature, *hOI*-MIECs started to be studied thoroughly as cathode materials for sodium-ion batteries, (e.g., Ppy/NaMnFe(CN)₆ (Li et al., 2015), PANI/NaNiFe(CN)₆ (Wang Z. et al., 2017), PEDOT/NaMnFe(CN)₆ (Wang et al., 2020), and Ppy/NaMnO₂ Lu et al., 2020). In the case of sodium-ion battery anode materials, the most frequent *hOI*-MIECs are based on metallic oxides such as PANI/SnO₂ (Zhao et al., 2015) and Ppy/SnO₂ (Yuan et al., 2018) and sulfides such as PANI/Co₃S₄ (Zhou et al., 2016) and Ppy/ZnS (Hou et al., 2017). It is interesting to mention that *hOI*-MIECs are also extensively used as cathodes of lithium-sulfur (Li-S) batteries such as PEDOT:PSS/S (Yang et al., 2011), Ppy/S (Han et al., 2019), and PANI/S (Wei et al., 2019). The study of MIECs as electrochemical transistors was reported long ago for typically doped Ppy (White et al., 1984), PANI (Paul et al., 1985), and PEDOT (Thackeray et al., 1985) conducting polymers, but the exploration of conducting polymers (principally PEDOT) doped with biocompatible materials such as hyaluronic acid, dextran sulfonate, heparin, pectin, guar gum, and deoxyribonucleic acid is rising fast in recent years, especially for bioelectronics purposes (Mantione et al., 2017; Tekoglu et al., 2019). In addition, a very recent report has shown that the preparation of an organic mixed-conducting particulate composite material based on PEDOT: PSS and chitosan enabled facile and effective electronic bonding between soft and rigid electronics, permitting recording of neurophysiological data at the resolution of individual neurons (Jastrzebska-Perfect et al., 2020). However, to the best of our knowledge, up to now, only carbon nanotubes (but no biocompatible inorganic nanoparticles) have been tested with organic MIECs to be evaluated for bioelectronics applications (Nie et al., 2015; Liu et al., 2019; Reddy et al., 2019; Yu et al., 2019).

CONCLUSIONS AND PERSPECTIVES

Herein, the state of the art of *hOI*-MIECs with special focus on charge carrier localization and transport at different regions including both bulk and interphase regions was discussed. In this particular case, we have mainly based our discussion by means of useful and versatile instrumental techniques such as micro-Raman and impedance spectroscopy, but other instrumental

techniques can be very useful and should be considered to gain more insight into the *hOI*-MIECs transport mechanism. There is no doubt that *hOI*-MIECs have shown to be very promising for different applications, ranging from more developed applications (e.g., lithium- and sodium-ion batteries) to more emerging applications (e.g., bioelectronics), as mentioned in the previous section. However, more work is still needed to understand the charge carrier transport mechanism of such complicated systems, in order to pursue the filling of the existent gap between fundamental knowledge and applications. In our opinion, *in situ/operando* monitoring of *hOI*-MIECs during working conditions is the ideal strategy to gain more insight into this field. However, as we have discussed in this mini-review, the complexity of these particular systems (biphasic by definition and sometimes intrinsically inhomogeneous) requires the rational design of more simple devices in order to make them accessible to a broader range of *in situ* characterization experiments. We think that the oncoming focus on these experiments is crucial to shed

some light on the structural and microstructural correlations of *hOI*-MIECs with the charge carrier transport mechanism.

AUTHOR CONTRIBUTIONS

MR, RF, and AM contributed to the conception and design of the study. DM and FP selected, compiled, and organized the literature references database. MR created the schematizations, adaptation of figure artwork, and wrote the first draft of the manuscript. DM, FP, RF, and AM wrote sections of the manuscript. All authors contributed to manuscript revision, read, and approved the submitted version.

ACKNOWLEDGMENTS

The authors wish to thank the support of Uruguayan CSIC, ANII, and PEDECIBA institutions as well as the Fondo Vaz Ferreira FVF-188 (D2C2-MEC) research project.

REFERENCES

- Aldebert, P., Audebert, P., Armand, M., Bidan, G., and Pineri, M. (1986). New chemical synthesis of mixed conductivity polymers. *J. Chem. Soc. Chem. Commun.* 1636–1638. doi: 10.1039/c39860001636
- Aoki, Y., Wiemann, C., Feyer, V., Kim, H.-S., Schneider, C. M., Ill-Yoo, H., et al. (2014). Bulk mixed ion electron conduction in amorphous gallium oxide causes memristive behavior. *Nat. Commun.* 5:473. doi: 10.1038/ncomms4473
- Atkinson, A., Baron, S. A., and Brandon, N. P. (2004). AC impedance spectra arising from mixed ionic electronic solid electrolytes. *J. Electrochem. Soc.* 151, E1E86–E1E93. doi: 10.1149/1.1690291
- Balaguer, M., Solís, C., and Serra, J. M. (2011). Study of the transport properties of the mixed ionic electronic conductor $Ce_{1-x}Tb_xO_{2-\delta}+Co(x = 0.1,0.2)$ and evaluation as oxygen-transport membrane. *Chem. Mater.* 23, 2333–2343. doi: 10.1021/cm103581w
- Barker, J., Pynenburg, R., Koksang, R., and Saidi, M. Y. (1996). An electrochemical investigation into the lithium insertion properties of Li_xCoO_2 . *Electrochim. Acta* 41, 2481–2488. doi: 10.1016/0013-4686(96)00036-9
- Barthet, C., and Guglielmi, M. (1995). Mixed electronic and ionic conductors: a new route to Nafion®-doped polyaniline. *J. Electroanal. Chem.* 388, 35–44. doi: 10.1016/0022-0728(94)03759-V
- Barthet, C., Guglielmi, M., and Baudry, P. (1997). A polyaniline + polyethylene oxide mixture as a composite polymer positive electrode in solid-state secondary batteries. *J. Electroanal. Chem.* 431, 145–152. doi: 10.1016/S0022-0728(97)00174-5
- Berthelot, R., Carlier, D., and Delmas, C. (2010). Electrochemical investigation of the $P_2-Na_xCoO_2$ phase diagram. *Nat. Mater.* 10, 74–80. doi: 10.1038/nmat2920
- Cai, S. D., Gao, C. H., Zhou, D. Y., Gu, W., and Liao, L. S. (2012). Study of hole-injecting properties in efficient, stable, and simplified phosphorescent organic light-emitting diodes by impedance spectroscopy. *ACS Appl. Mater. Interfaces* 4, 312–316. doi: 10.1021/am2013568
- Cao, F., and Prakash, J. (2002). A comparative electrochemical study of $LiMn_2O_4$ spinel thin-film and porous laminate. *Electrochim. Acta* 47, 1607–1613. doi: 10.1016/S0013-4686(01)00884-2
- Chatterjee, K., Mitra, M., Kargupta, K., Ganguly, S., and Banerjee, D. (2013). Synthesis, characterization and enhanced thermoelectric performance of structurally ordered cable-like novel polyaniline-bismuth telluride nanocomposite. *Nanotechnology* 24:215703. doi: 10.1088/0957-4484/24/21/215703
- Chen, C.-C., Huang, B.-C., Lin, M.-S., Lu, Y.-J., Cho, T.-Y., Chang, C.-H., et al. (2010). Impedance spectroscopy and equivalent circuits of conductively doped organic hole-transport materials. *Org. Electron.* 11, 1901–1908. doi: 10.1016/j.orgel.2010.09.005
- Chen, D., Ding, D., Li, X., Waller, G., Xiong, X., El-Sayed, M., et al. (2015). Probing the charge storage mechanism of a pseudocapacitive MnO_2 electrode using *in operando* Raman spectroscopy. *Chem. Mater.* 27, 6608–6619. doi: 10.1021/acs.chemmater.5b03118
- Cheng, C. H. W., Lin, F., and Lonergan, M. C. (2005). Charge transport in a mixed ionically/electronically conducting, cationic, polyacetylene ionomer between ion-blocking electrodes. *J. Phys. Chem. B* 109, 10168–10178. doi: 10.1021/jp0505431
- Crispin, X., Jakobsson, F. L. E., Crispin, A., Grim, P. C. M., Andersson, P., Volodin, A., et al. (2006). The origin of the high conductivity of poly(3,4-ethylenedioxythiophene)-poly(styrenesulfonate) (PEDOT-PSS) plastic electrodes. *Chem. Mater.* 18, 4354–4360. doi: 10.1021/cm061032+
- Cui, L., Shen, J., Cheng, F., Tao, Z., and Chen, J. (2011). SnO_2 nanoparticles@polypyrrole nanowires composite as anode materials for rechargeable lithium-ion batteries. *J. Power Sources* 196:2195. doi: 10.1016/j.jpowsour.2010.09.075
- Della Santa, A., De Rossi, D., and Mazzoldi, A. (1997). Performance and work capacity of a polypyrrole conducting polymer linear actuator. *Synthetic Metals* 90, 93–100. doi: 10.1016/S0379-6779(97)81256-8
- Doeff, M. M., Ma, Y., Visco, S. J., and De Jonghe, L. C. (1993). Electrochemical insertion of sodium into carbon. *J. Electrochem. Soc.* 140, L1L69–L1L70. doi: 10.1149/1.2221153
- Dokko, K., Mohamedi, M., Fujita, Y., Itoh, T., Nishizawa, M., Umeda, M., et al. (2001). Kinetic characterization of single particles of $LiCoO_2$ by AC impedance and potential step methods. *J. Electrochem. Soc.* 148, A4A22–A4A26. doi: 10.1149/1.1359197
- Dokko, K., Shi, Q., Stefan, I. C., and Scherson, D. A. (2003). *In situ* Raman spectroscopy of single microparticle Li^+ -intercalation electrodes. *J. Phys. Chem. B* 107, 12549–12554. doi: 10.1021/jp034977c
- Dong, B. X., Nowak, C., Onorato, J. W., Strzalka, J., Escobedo, F. A., Luscombe, C. K., et al. (2019). Influence of side-chain chemistry on structure and ionic conduction characteristics of polythiophene derivatives: a computational and experimental study. *Chem. Mater.* 31, 1418–1429. doi: 10.1021/acs.chemmater.8b05257
- Fedorokova, A., Alejos, A. N., Romero, P. G., Orinakovic, R., and Kaniansky, D. (2010). Structural and electrochemical studies of PPy/PEG-LiFePO₄ cathode material for Li-ion batteries. *Electrochim. Acta* 55, 943–947. doi: 10.1016/j.electacta.2009.09.060
- Flores, E., Novák, P., and Berg, E. J. (2018). *In situ* and *operando* Raman spectroscopy of layered transition metal oxides for Li-ion battery cathodes. *Front. Energy Res.* 6:82. doi: 10.3389/fenrg.2018.00082
- Francis, C., Fazzi, D., Grimm, S. B., Paulus, F., Beck, S., Hillebrandt, S., et al. (2017). Raman spectroscopy and microscopy of electrochemically and

- chemically doped high-mobility semiconducting polymers. *J. Mater. Chem. C* 5, 6176–6184. doi: 10.1039/C7TC01277B
- Fu, Y., and Manthiram, A. (2012). Enhanced cyclability of lithium–sulfur batteries by a polymer acid-doped polypyrrole mixed ionic–electronic conductor. *Chem. Mater.* 24, 3081–3087. doi: 10.1021/cm301661y
- Furukawa, Y. (1996). Electronic absorption and vibrational spectroscopies of conjugated conducting polymers. *J. Phys. Chem.* 100, 15644–15653. doi: 10.1021/jp960608n
- Ghosh, S., and Inganäs, O. (2000). Networks of electron-conducting polymer in matrices of ion-conducting polymers applications to fast electrodes. *Electrochem. Solid-State Lett.* 3, 213–215. doi: 10.1149/1.1391005
- Glaudell, A. M., Cochran, J. E., Patel, S. N., and Chabiny, M. L. (2015). Impact of the doping method on conductivity and thermopower in semiconducting polythiophenes. *Adv. Energy Mater.* 5:1401072. doi: 10.1002/aenm.201401072
- Gómez-Romero, P., and Lira-Cantú, M. (1997). Hybrid organic-inorganic electrodes: the molecular material formed between polypyrrole and the phosphomolybdate anion. *Adv. Mater.* 9, 144–147. doi: 10.1002/adma.19970090210
- Goodenough, J. B. (2000). Oxide-ion conductors by design. *Nature* 404, 821–823. doi: 10.1038/35009177
- Guizard, C., Bac, A., Barboiu, M., and Hovnanian, N. (2001). Hybrid organic-inorganic membranes with specific transport properties: applications in separation and sensors technologies. *Separat. Purification Technol.* 25, 167–180. doi: 10.1016/S1383-5866(01)00101-0
- Han, P., Chung, S.-H., and Manthiram, A. (2019). Designing a high-loading sulfur cathode with a mixed ionic-electronic conducting polymer for electrochemically stable lithium-sulfur batteries. *Energy Storage Mater.* 17, 317–324. doi: 10.1016/j.ensm.2018.11.002
- Han, S., Ul Hassan Alvi, N., Granlöv, L., Granberg, H., Berggren, M., Fabiano, S., et al. (2019). A multiparameter pressure-temperature-humidity sensor based on mixed ionic-electronic cellulose aerogels. *Adv. Sci.* 6:1802128. doi: 10.1002/advs.201802128
- Hou, T., Tang, G., Sun, X., Cai, S., Zheng, C., and Hu, W. (2017). Perchlorate ion doped polypyrrole coated ZnS sphere composites as a sodium-ion battery anode with superior rate capability enhanced by pseudocapacitance. *RSC Adv.* 7, 43636–43641. doi: 10.1039/C7RA07901J
- Huggins, R. A. (2002). Simple method to determine electronic and ionic components of the conductivity in mixed conductors, a review. *Ionics* 8, 300–313. doi: 10.1007/BF02376083
- Huguénin, F., Ferreira, M., Zucolotto, V., Nart, F. C., Torresi, R. M., Oliveira, J. R., et al. (2004). Molecular-level manipulation of V₂O₅/polyaniline layer-by-layer films to control electrochromogenic and electrochemical properties. *Chem. Mater.* 16, 2293–2299. doi: 10.1021/cm035171s
- Inal, S., Rivnay, J., Suii, A.-O., Malliaras, G. G., and McCulloch, I. (2018). Conjugated polymers in bioelectronics. *Acc. Chem. Res.* 51, 1368–1376. doi: 10.1021/acs.accounts.7b00624
- Irvine, J. T. S., Sinclair, D. C., and West, A. R. (1990). Electroceramics: characterization by impedance spectroscopy. *Adv. Mater.* 2, 132–138. doi: 10.1002/adma.19900020304
- Jacobs, I. E., Aasen, E. W., Oliveira, J. L., Fonseca, T. N., Roehling, J. D., Li, J., et al. (2016). Comparison of solution-mixed and sequentially processed P3HT:F4TCNQ films: effect of doping-induced aggregation on film morphology. *J. Mater. Chem. C* 4, 3454–3466. doi: 10.1039/C5TC04207K
- Jamnik, J., and Maier, J. (1999). Treatment of the impedance of mixed conductors, equivalent circuit model and explicit approximate solutions. *J. Electrochem. Soc.* 146, 4183–4188. doi: 10.1149/1.1392611
- Jastrzebska-Perfect, P., Spyropoulos, G. D., Cea, C., Zhao, Z., Rauhala, O. J., Viswanathan, A., et al. (2020). Mixed-conducting particulate composites for soft electronics. *Sci. Adv.* 6:eaa26767. doi: 10.1126/sciadv.aaz6767
- Javier, A. E., Patel, S. N., Hallinan, Jr D. T., Srinivasan, V., and Balsara, N.P. (2011). Simultaneous electronic and ionic conduction in a block copolymer: application in lithium battery electrodes. *Angew. Chem. Int. Ed.* 50:9848. doi: 10.1002/anie.201102953
- Ju, S. H., Kang, I. S., Lee, Y. S., Shin, D. K., Kim, S., Shin, K., et al. (2014). Improvement of the cycling performance of LiNi_{0.6}Co_{0.2}Mn_{0.2}O₂ cathode active materials by a dual-conductive polymer coating. *ACS Appl. Mater. Interfaces* 6, 2546–2552. doi: 10.1021/am404965p
- Judeinstein, P., and Sanchez, C. (1996). Hybrid organic-inorganic materials: a land of multidisciplinary. *J. Mater. Chem.* 6, 511–525. doi: 10.1039/JM9960600511
- Jung, I. H., Hong, C. T., Lee, U.-H., Kang, Y. H., Jang, K.-S., and Cho, S. Y. (2017). High thermoelectric power factor of a diketopyrrolopyrrole-based low bandgap polymer via finely tuned doping engineering. *Sci. Rep.* 7:44704. doi: 10.1038/srep44704
- Kang, I. S., Lee, Y. S., and Kim, D. W. (2014). Improved cycling stability of lithium electrodes in rechargeable lithium batteries. *J. Electrochem. Soc.* 161, A5A3–A5A7. doi: 10.1149/2.029401jes
- Kim, G. H., Shao, L., Zhang, K., and Pipe, K. P. (2013). Engineered doping of organic semiconductors for enhanced thermoelectric efficiency. *Nat. Mater.* 12:719. doi: 10.1038/nmat3635
- Kloster, G. M., Thomas, J. A., Brazis, P. W., Kannewurf, C. R., and Shriver, D. F. (1996). Synthesis, characterization, and transport properties of new mixed ionic-electronic conducting V₂O₅-polymer electrolyte xerogel nanocomposites. *Chem. Mater.* 8, 2418–2420. doi: 10.1021/cm9603361
- Kumar, R., Pillai, R. G., Pekas, N., Wu, Y., and McCreery, R. L. (2012). Spatially resolved raman spectroelectrochemistry of solid-state polythiophene/violon memory devices. *J. Am. Chem. Soc.* 134, 14869–14876. doi: 10.1021/ja304458s
- Kumar, S. R. S., Kurra, N., and Alshareef, H. N. (2016). Enhanced high temperature thermoelectric response of sulphuric acid treated conducting polymer thin films. *J. Mater. Chem. C* 4, 215–221. doi: 10.1039/C5TC03145A
- Le Bideau, J., Viau, L., and Vioux, A. (2011). Ionogels, ionic liquid based hybrid materials. *Chem. Soc. Rev.* 40, 907–925. doi: 10.1039/C0CS00059K
- Lee, J. S., Jamnik, J., and Maier, J. (2009). Generalized equivalent circuits for mixed conductors: silver sulfide as a model system. *Monatshfte für Chemie* 140, 1113–1119. doi: 10.1007/s00706-009-0130-x
- Lee, S. H., Park, H., Kim, S., Son, W., Cheong, I. W., and Kim, J. H. (2014). Transparent and flexible organic semiconductor nanofilms with enhanced thermoelectric efficiency. *J. Mater. Chem. A* 2, 7288–7294. doi: 10.1039/C4TA00700J
- Levasseur, S., Ménétrier, M., and Delmas, C. (2002). On the dual effect of Mg doping in LiCoO₂ and Li1+ δ CoO₂: structural, electronic properties, and 7Li MAS NMR Studies. *Chem. Mater.* 14 3584–3590. doi: 10.1021/cm021107j
- Li, J., and Khan, I. M. (1991). Mixed (electronic and ionic) conductive solid polymer matrix, synthesis and properties of poly(2,5,8,11,14,17,20,23-octaaxapentacosylmethacrylate)-block-poly(4-vinylpyridine). *Makromol. Chem.* 192, 3043–3050. doi: 10.1002/macp.1991.021921219
- Li, W.-J., Chou, S.-L., Wang, J.-Z., Wang, J.-L., Gu, Q.-F., Liu, H.-K., et al. (2015). Multifunctional conducting polymer coated NaLa+xMnFe(CN)₆ cathode for sodium-ion batteries with superior performance via a facile and one-step chemistry approach. *Nano Energy* 13, 200–207. doi: 10.1016/j.nanoen.2015.02.019
- Lim, E., Peterson, K. A., Su, G. M., and Chabiny, M. L. (2018). Thermoelectric properties of poly(3-hexylthiophene) (P3HT) doped with 2,3,5,6-tetrafluoro-7,8-tetracyanoquinodimethane (F4TCNQ) by vapor-phase infiltration. *Chem. Mater.* 30, 998–1010. doi: 10.1021/acs.chemmater.7b04849
- Lin, Y., Fang, S., Su, D., Brinkman, K. S., and Chen, F. (2015). Enhancing grain boundary ionic conductivity in mixed ionic–electronic conductors. *Nat. Commun.* 6:6824. doi: 10.1038/ncomms7824
- Liu, C., Wang, W., Li, Y., Cui, F., Xie, C., Zhu, L., et al. (2019). PMWCNT/PVDF ultrafiltration membranes with enhanced antifouling properties intensified by electric field for efficient blood purification. *J. Membr. Sci.* 576, 48–58. doi: 10.1016/j.memsci.2019.01.015
- Liu, J., Davis, N. R., Liu, D. S., and Hammond, P. T. (2012). Highly transparent mixed electron and proton conducting polymer membranes. *J. Mater. Chem.* 22:15534. doi: 10.1039/c2jm32296j
- Liu, L. L., Wang, X. J., Zhu, Y. S., Hu, C. L., Wu, Y. P., and Holze, R. (2013). Polypyrrole-coated LiV₃O₈-nanocomposites with good electrochemical performance as anode material for aqueous rechargeable lithium batteries. *J. Power Sources* 224, 290–294. doi: 10.1016/j.jpowsour.2012.09.100
- Liu, Q., Hu, Z., Chen, M., Zou, C., Jin, H., Wang, S., et al. (2020). The cathode choice for commercialization of sodium-ion batteries: layered transition metal oxides versus prussian blue analogs. *Adv. Funct. Mater.* 30:1909530. doi: 10.1002/adfm.201909530
- Lu, D., Yao, Z. J., Li, Y. Q., Zhong, Y., Wang, X. L., Xie, D., et al. (2020). Sodium-rich manganese oxide porous microcubes with polypyrrole coating as a superior

- cathode for sodium ion full batteries. *J. Colloid Interface Sci.* 565, 218–226. doi: 10.1016/j.jcis.2020.01.023
- Lu, Z., and Dahn, J. R. (2001). *In situ* X-ray diffraction study of P_2 -Na-2/3[Ni_{1/3}Mn_{2/3}]O-2. *J. Electrochem. Soc.* 148, A1A225–A1A229. doi: 10.1149/1.1407247
- Maier, J. (2005). Nanoionics: ion transport and electrochemical storage in confined systems. *Nature Materials* 4, 805–815. doi: 10.1038/nmat1513
- Mantione, D., del Agua, I., Sanchez-Sanchez, A., and Mecerreyes, D. (2017). Poly(3,4-ethylenedioxythiophene) (PEDOT) derivatives: innovative conductive polymers for bioelectronics. *Polymers* 9:354. doi: 10.3390/polym9080354
- Mengistie, D. A., Chen, C.-H., Boopathi, K. M., Pranoto, F. W., Li, L.-J., and Chu, C.-W. (2015). Enhanced thermoelectric performance of pedot:pss flexible bulky papers by treatment with secondary dopants. *ACS Appl. Mater. Interfaces* 7, 94–100. doi: 10.1021/am507032e
- Mengistie, D. A., Wang, P.-C., and Chu, C.-W. (2013). Effect of molecular weight of additives on the conductivity of pedot:pss and efficiency for ito-free organic solar cells. *J. Mater. Chem. A* 1, 9907–9915. doi: 10.1039/c3ta11726j
- Miyatani, S. (1973). Electronic and ionic conduction in (AgxCu_{1-x})₂Se. *J. Phys. Soc. Jap.* 34, 423–432. doi: 10.1143/JPSJ.34.423
- Mombrú, D., Romero, M., Faccio, R., Castiglioni, J., and Mombrú, A. W. (2017a). *In situ* growth of ceramic quantum dots in polyaniline host via water vapor flow diffusion as potential electrode materials for energy applications. *J. Solid State Chem.* 250, 60–67. doi: 10.1016/j.jssc.2017.03.016
- Mombrú, D., Romero, M., Faccio, R., and Mombrú, A. W. (2017b). Raman and impedance spectroscopy under applied dc bias insights on the electrical transport for donor:acceptor nanocomposites based on poly(vinyl carbazole) and TiO₂ quantum dots. *J. Phys. Chem. C* 121, 23383–23391. doi: 10.1021/acs.jpcc.7b08400
- Mombrú, D., Romero, M., Faccio, R., and Mombrú, A. W. (2017c). From positive to negative magnetoresistance behavior at low applied magnetic fields for polyaniline:titania quantum dot nanocomposites. *J. Appl. Phys.* 121:245106. doi: 10.1063/1.4989831
- Mombrú, D., Romero, M., Faccio, R., and Mombrú, A. W. (2018). Raman microscopy insights on the out-of-plane electrical transport of carbon nanotube-doped PEDOT:PSS electrodes for solar cell applications. *J. Phys. Chem. B* 122, 2694–2701. doi: 10.1021/acs.jpcc.8b00317
- Mombrú, D., Romero, M., Faccio, R., and Mombrú, A. W. (2019). Transition from positive to negative electrical resistance response under humidity conditions for PEDOT:PSS-MoS₂ nanocomposite thin films. *J. Mater. Sci.* 30, 5959–5964. doi: 10.1007/s10854-019-00895-z
- Murthy, A., and Manthiram, A. (2011). Highly water-dispersible, mixed ionic-electronic conducting, polymer acid-doped polyanilines as ionomers for direct methanol fuel cells. *Chem. Commun.* 47, 6882–6884. doi: 10.1039/c1cc11473e
- Nanda, J., Remillard, J., O'Neill, A., Bernardi, D., Ro, T., Nietering, K. E., et al. (2011). Local state-of-charge mapping of lithium-ion battery electrodes. *Adv. Funct. Mater.* 21, 3282–3290. doi: 10.1002/adfm.201100157
- Nie, C., Ma, L., Xia, Y., He, C., Deng, J., Wang, L., et al. (2015). Novel heparin mimicking polymer brush grafted carbon nanotube/PES composite membranes for safe and efficient blood purification. *J. Membr. Sci.* 475, 455–468. doi: 10.1016/j.memsci.2014.11.005
- Nightingale, J., Wade, J., Moia, D., Nelson, J., and Kim, J.-S. (2018). Impact of molecular order on polaron formation in conjugated polymers. *J. Phys. Chem. C* 122, 29129–29140. doi: 10.1021/acs.jpcc.8b09706
- Nigrey, P. J., Macdiarmid, A. G., and Heeg, A. J. (1978). Electrochemistry of polyacetylene, (CH): electrochemical doping of (CH)_x films to the metallic state. *J. Chem. Soc. Chem. Commun.* 594–595. doi: 10.1039/c39790000594
- Nishi, T., Nakai, H., and Kita, A. (2013). Visualization of the state-of-charge distribution in a LiCoO₂ cathode by *in situ* raman imaging. *J. Electrochem. Soc.* 160, A1A785–A1A788. doi: 10.1149/2.061310jes
- Nowy, S., Ren, W., Elschner, A., Lovenich, W., and Brutting, W. (2010). Impedance spectroscopy as a probe for the degradation of organic light-emitting diodes. *J. Appl. Phys.* 107:054501. doi: 10.1063/1.3294642
- Onorato, J. W., and Luscombe, C. K. (2019). Morphological effects on polymeric mixed ionic/electronic conductors. *Mol. Syst. Des. Eng.* 4, 310–324. doi: 10.1039/C8ME00093J
- Park, M., Zhang, X., Chung, M., Less, G. B., and Sastry, A. M. (2010). A review of conduction phenomena in Li-ion batteries. *J. Power Sources* 195, 7904–7929. doi: 10.1016/j.jpowsour.2010.06.060
- Patel, S. N., Javier, A. E., Stone, G. M., Mullin, S. A., and Balsara, N. P. (2012). Simultaneous conduction of electronic charge and lithium ions in block copolymers. *ACS Nano* 6, 1589–1600. doi: 10.1021/nn2045664
- Paul, E. W., Ricco, A. J., and Wrighton, M. S. (1985). Resistance of polyaniline films as a function of electrochemical potential and the fabrication of polyaniline-based microelectronic devices. *J. Phys. Chem.* 1985, 1441–1447. doi: 10.1021/j100254a028
- Paulsen, B. D., Tybrandt, K., Stavrinidou, E., and Rivnay, J. (2020). Organic mixed ionic–electronic conductors. *Nat. Mater.* 19, 13–26. doi: 10.1038/s41563-019-0435-z
- Pignatelli, F., Romero, M., Castiglioni, J., Faccio, R., and Mombrú, A. W. (2019b). Novel synergistic *in situ* synthesis of lithium-ion poly(ethylene citrate)-TiO₂ nanocomposites as promising fluorine-free solid polymer electrolytes for lithium batteries. *J. Phys. Chem. Solids* 135:109082. doi: 10.1016/j.jpcs.2019.109082
- Pignatelli, F., Romero, M., Estéves, M., Fernández-Werner, L., Faccio, R., and Mombrú, A. W. (2019a). Lithium titanate nanotubes as active fillers for lithium-ion polyacrylonitrile solid polymer electrolytes. *Ionics* 25, 2607–2614. doi: 10.1007/s11581-018-2768-z
- Pignatelli, F., Romero, M., Faccio, R., Fernández-Werner, L., and Mombrú, A. W. (2018). Enhancement of lithium-ion transport in poly(acrylonitrile) with hydrogen titanate nanotube fillers as solid polymer electrolytes for lithium-ion battery applications. *J. Phys. Chem. C* 122, 1492–1499. doi: 10.1021/acs.jpcc.7b10725
- Pingel, P., and Neher, D. (2013). Comprehensive picture of p-type doping of P3HT with the molecular acceptor F4TCNQ. *Phys. Rev. B* 87:115209. doi: 10.1103/PhysRevB.87.115209
- Qu, S., Yao, Q., Shi, W., Wang, W., and Chen, L. (2016). The influence of molecular configuration on the thermoelectrical properties of poly(3-hexylthiophene). *J. Electron. Mater.* 45:8. doi: 10.1007/s11664-015-4045-5
- Reddy, S., Xiao, Q., Liu, H. Q., Li, C. P., Chen, S. F., Wang, C., et al. (2019). Bionanotube/poly(3,4-ethylenedioxythiophene) nanohybrid as an electrode for the neural interface and dopamine sensor. *ACS Appl. Mater. Interfaces* 11, 18254–18267. doi: 10.1021/acsami.9b04862
- Renna, L. A., Lenef, J. D., Bag, M., and Venkataraman, D. (2017). Mixed ionic–electronic conduction in binary polymer nanoparticle assemblies. *Adv. Mater. Interfaces* 1700397, 10397–8. doi: 10.1002/admi.201700397
- Riess, I. (2000). Polymeric mixed ionic electronic conductors. *Solid State Ionics* 136–137, 1119–1130. doi: 10.1016/S0167-2738(00)00607-X
- Riess, I. (2003). Mixed ionic-electronic conductors-material properties and applications. *Solid State Ionics* 157, 1–17. doi: 10.1016/S0167-2738(02)00182-0
- Rivnay, J., Inal, S., Collins, B. A., Sessolo, M., Stavrinidou, E., Strakosas, X., et al. (2016). Structural control of mixed ionic and electronic transport in conducting polymers. *Nat. Commun.* 7:11287. doi: 10.1038/ncomms11287
- Romero, M., Faccio, R., Vázquez, S., and Mombrú, A. W. (2016). Enhancement of lithium conductivity and evidence of lithium dissociation for LLTO-PMMA nanocomposite electrolyte. *Mater. Lett.* 172, 1–5. doi: 10.1016/j.matlet.2016.02.128
- Roussel, F., Chen, Yu King, R., Kuriakose, M., Depriester, M., Hadj-Sahraoui, A., Gors, C., et al. (2015). Electrical and thermal transport properties of polyaniline/silver composites and their use as thermoelectric materials. *Synth. Met.* 199, 196–204. doi: 10.1016/j.synthmet.2014.11.020
- Saïdi, M. Y., Barker, J., and Koksang, R. (1996). Thermodynamic and kinetic investigation of lithium insertion in the Li_{1-x}Mn₂O₄ spinel phase. *J. Solid State Chem.* 122, 195–199. doi: 10.1006/jssc.1996.0101
- Sanjeeva Murthy, N. (2016). “Chapter 2: x-ray diffraction from polymers,” in *Polymer Morphology: Principles, Characterization, and Processing, 1st Edn*, ed Qipeng Guo (Hoboken, NJ: John Wiley & Sons, Inc), 14–36. doi: 10.1002/9781118892756.ch2
- Sauvage, F., Laffont, L., Tarascon, J. M., and Baudrin, E. (2007). Study of the insertion/deinsertion mechanism of sodium into Na_{0.44}MnO₂. *Inorg. Chem.* 46, 3289–3294. doi: 10.1021/ic0700250
- Scrosati, B., Croce, F., and Persi, L. (2000). Impedance spectroscopy study of PEO-based nanocomposite polymer electrolytes. *J. Electrochem. Soc.* 147, 1718–1721. doi: 10.1149/1.1393423

- Sengodu, P., and Deshmukh, A. (2015). Conducting polymers and their inorganic composites for advanced Li-ion batteries: a review. *RSC Adv.* 5, 42109–42130. doi: 10.1039/C4RA17254J
- Sengwa, R. J., and Dhatwarwal, P. (2020). Predominantly chain segmental relaxation dependent ionic conductivity of multiphase semicrystalline PVDF/PEO/LiClO₄ solid polymer electrolytes. *Electrochim. Acta* 338:135890. doi: 10.1016/j.electacta.2020.135890
- Shao, Z., and Haile, S. M. (2004). A high-performance cathode for the next generation of solid-oxide fuel cells. *Nature* 431, 170–173. doi: 10.1038/nature02863
- Shi, Y., Zhou, X., Zhang, J., Bruck, A. M., Bond, A. C., Marschilok, A. C., et al. (2017). Nanostructured conductive polymer gels as a general framework material to improve electrochemical performance of cathode materials in Li-ion batteries. *Nano Lett.* 17, 1906–1914. doi: 10.1021/acs.nanolett.6b05227
- Shin, J. H., and Passerini, S. (2004). PEO-LiN(SO₂CF₂CF₃)₂ polymer electrolytes V. Effect of fillers on ionic transport properties. *J. Electrochem. Soc.* 151, A2A38–A2A45.
- Stavrinidou, E., Leleux, P., Rajaona, H., Khodagholy, D., Rivnay, J., Lindau, M., et al. (2013). Direct measurement of ion mobility in a conducting polymer. *Adv. Mater.* 25, 4488–4493. doi: 10.1002/adma.201301240
- Takano, T., Masunaga, H., Fujiwara, A., Okuzaki, H., and Sasaki, T. (2012). Pedot nanocrystal in highly conductive pedot:pss polymer films. *Macromolecules* 45, 3859–3865. doi: 10.1021/ma300120g
- Tang, W., Gao, X. W., Zhu, Y. S., Yue, Y. B., Shi, Y., Wu, Y. P., et al. (2012b). A hybrid of V₂O₅ nanowires and MWCNTs coated with polypyrrole as an anode material for aqueous rechargeable lithium batteries with excellent cycling performance. *J. Mater. Chem.* 22, 20143–20145. doi: 10.1039/c2jm34563c
- Tang, W., Liu, L., Zhu, Y., Sun, H., Wu, Y., and Zhu, K. (2012a). An aqueous rechargeable lithium battery of excellent rate capability based on a nanocomposite of MoO₃ coated with PPy and LiMn₂O₄. *Energy Environ. Sci.* 5, 6909–6913. doi: 10.1039/c2ee21294c
- Tekoglu, S., Wielend, D., Scharber, M. C., Sariciftci, N. S., and Yumusak, C. (2019). Conducting polymer-based biocomposites using deoxyribonucleic acid (DNA) as counterion. *Adv. Mater. Technol.* 5:1900699. doi: 10.1002/admt.201900699
- Tevar, A. D., and Whitacre, J. F. (2010). Relating synthesis conditions and electrochemical performance for the sodium intercalation compound Na₄Mn₉O₁₈ in aqueous electrolyte. *J. Electrochem. Soc.* 157, A8A70–A8A75. doi: 10.1149/1.3428667
- Thackeray, J. W., White, H. S., and Wrighton, M. S. (1985). Poly(3-methylthiophene)-coated electrodes: optical and electrical properties as a function of redox potential and amplification of electrical and chemical signals using poly(3-methylthiophene)-based microelectrochemical transistors. *J. Phys. Chem.* 1985, 5133–5140. doi: 10.1021/j100269a048
- Thackeray, M. M. (1997). Manganese oxides for lithium batteries. *Prog. Solid State Chem.* 25, 1–71. doi: 10.1016/S0079-6786(97)81003-5
- Tian, F., Liu, L., Yang, Z., Wang, X., Chen, Q., and Wang, X. (2011). Electrochemical characterization of a LiV₃O₈-polypyrrole composite as a cathode material for lithium ion batteries. *Mater. Chem. Phys.* 127, 151–155. doi: 10.1016/j.matchemphys.2011.01.051
- Udo, L., Elisabeth, M., Nicola, N., and Jurg, D. (2009). Microscopical investigations of pedot:pss thin films. *Adv. Funct. Mater.* 19, 1215–1220. doi: 10.1002/adfm.200801258
- Vadivel Murugan, A., Muraliganth, T., and Manthiram, A. (2008). Rapid microwave-solvothermal synthesis of phospho-olivine nanorods and their coating with a mixed conducting polymer for lithium ion batteries. *Electrochem. Commun.* 10, 903–906. doi: 10.1016/j.elecom.2008.04.004
- Vorotyntsev, M. A., Deslouis, C., Musiani, M. M., Tribollet, B., and Aoki, K. (1999). Transport across an electroactive polymer film in contact with media allowing both ionic and electronic interfacial exchange. *Electrochim. Acta* 44, 2105–2115. doi: 10.1016/S0013-4686(98)00318-1
- Wachsman, E. D., and Lee, K. T. (2011). Lowering the temperature of solid oxide fuel cells. *Science* 334, 935–939. doi: 10.1126/science.1204090
- Wang, G. J., Yang, L. C., Qu, Q. T., Wang, B., Wu, Y. P., and Holze, R. (2010). An aqueous rechargeable lithium battery based on doping and intercalation mechanisms. *J. Solid State Electrochem.* 14:865. doi: 10.1007/s10008-009-0869-3
- Wang, W., Chen, C., Tollan, C., Yang, F., Qin, Y., and Knez, M. (2017). Efficient and controllable vapor to solid doping of the polythiophene P3HT by low temperature vapor phase infiltration. *J. Mater. Chem. C* 5, 2686–2694. doi: 10.1039/C6TC05544C
- Wang, X., Wang, B., Tang, Y., Xu, B. B., Liang, C., Yana, M., et al. (2020). Manganese hexacyanoferrate reinforced by PEDOT coating towards high-rate and long-life sodium-ion battery cathode. *J. Mater. Chem. A* 8, 3222–3227. doi: 10.1039/C9TA12376H
- Wang, Z., Liu, Y., Wu, Z., Guan, G., Zhang, D., Zheng, H., et al. (2017). A string of nickel hexacyanoferrate nanocubes coaxially grown on a CNT@bipolar conducting polymer as a high-performance cathode material for sodium-ion batteries. *Nanoscale* 9, 823–831. doi: 10.1039/C6NR08765E
- Watanabe, M. (1996). Molecular design of ion and ion/electron mixed conducting polymers. *Macromol. Symp.* 105, 229–233. doi: 10.1002/masy.19961050133
- Wei, Y., Yan, Y., Zou, Y., Shi, M., Deng, Q., Zhao, N., et al. (2019). The ternary conductive polymer coated S/BDPC composite cathode for enhancing the electrochemical prospects in Li-S batteries. *Surface Coatings Technol.* 358, 560–566. doi: 10.1016/j.surfcoat.2018.11.038
- White, H. S., Kittleson, G. P., and Wrighton, M. S. (1984). Chemical derivatization of an array of three gold microelectrodes with polypyrrole: fabrication of a molecule-based transistor. *J. Am. Chem. Soc.* 11, 5375–5377. doi: 10.1021/ja00330a070
- Xiang, X., Zhang, K., and Chen, J. (2015). Recent advances and prospects of cathode materials for sodium-ion batteries. *Adv. Mater.* 27, 5343–5364. doi: 10.1002/adma.201501527
- Yamamoto, J., and Furukawa, Y. (2015). Electronic and vibrational spectra of positive polarons and bipolarons in regioregular poly(3-hexylthiophene) doped with ferric chloride. *J. Phys. Chem. B* 119, 4788–4794. doi: 10.1021/jp512654b
- Yang, T., Zheng, J., Cheng, Q., Hu, Y.-Y., and Chan, C. K. (2017). Composite polymer electrolytes with 6th Li₇La₃Zr₂O₁₂ garnet-type nanowires as ceramic fillers: mechanism of conductivity enhancement and role of doping and morphology. *ACS Appl Mater Interfaces* 9, 21773–21780. doi: 10.1021/acsami.7b03806
- Yang, Y., Yu, G., Cha, J. J., Wu, H., Vosgueritchian, M., Yao, Y., et al. (2011). Improving the performance of lithium-sulfur batteries by conductive polymer coating. *ACS Nano* 5, 9187–9193. doi: 10.1021/nn203436j
- Yokota, I. (1961). On the theory of mixed conduction with special reference to conduction in silver sulfide group semiconductors. *J. Phys. Soc. Jap.* 16, 2213–2223. doi: 10.1143/JPSJ.16.2213
- Yu, X., Zhu, Y., Cheng, C., Zhang, T., Wang, X., and Hsiao, B. S. (2019). Novel thin-film nanofibrous composite membranes containing directional toxin transport nanochannels for efficient and safe hemodialysis application. *J. Membr. Sci.* 582, 151–163. doi: 10.1016/j.memsci.2019.04.006
- Yuan, J., Hao, Y., Zhang, X., and Li, X. (2018). Sandwiched CNT@SnO₂@PPy nanocomposites enhancing sodium storage. *Colloids Surfaces A* 555, 795–801. doi: 10.1016/j.colsurfa.2018.07.023
- Yuan, L., Wang, J., Chew, S. Y., Chen, J., Guo, Z. P., Zhao, L., et al. (2007). Synthesis and characterization of SnO₂-polypyrrole composite for lithium-ion battery. *J. Power Sources* 174, 1183–1187. doi: 10.1016/j.jpowsour.2007.06.179
- Zhang, F., Cao, H., Yue, D., Zhang, J., and Qu, M. (2012). Enhanced anode performances of polyaniline-TiO₂-reduced graphene oxide nanocomposites for lithium ion batteries. *Inorg. Chem.* 2012, 9544–9551. doi: 10.1021/ic301378j
- Zhang, K., Davis, M., Qiu, J., Hope-Weeks, L., and Wang, S. (2012). Thermoelectric properties of porous multi-walled carbon nanotube/polyaniline core/shell nanocomposites. *Nanotechnology* 23:385701. doi: 10.1088/0957-4484/23/38/385701
- Zhang, Q., Sun, Y., Xu, W., and Zhu, D. (2012). Thermoelectric energy from flexible P3HT films doped with a ferric salt of triflimide anions. *Energy Environ. Sci.* 5, 9639–9644. doi: 10.1039/c2ee23006b
- Zhang, Q., Wang, W., Li, J., Zhu, J., Wang, L., Zhu, M., et al. (2013). Preparation and thermoelectric properties of multi-walled carbon nanotube/polyaniline hybrid nanocomposites. *J. Mater. Chem. A* 1, 12109–12114. doi: 10.1039/c3ta12353g
- Zhang, X. W., Wang, C., Appleby, A. J., and Little, F. E. (2002). Composite doped emeraldine-polyethylene oxide-bonded lithium-ion nano-tin anodes with electronic-ionic mixed conduction. *Solid State Ionics* 150, 383–389. doi: 10.1016/S0167-2738(02)00522-2
- Zhang, Z. J., Wang, J. Z., Chou, S. L., Liu, H. K., Ozawa, K., and Li, H. (2013). Polypyrrole-coated α-LiFeO₂O nanocomposite with enhanced

- electrochemical properties for lithium-ion batteries. *Electrochim. Acta* 108, 820–826. doi: 10.1016/j.electacta.2013.06.130
- Zhao, X., Zhang, Z., Yang, F., Fu, Y., Lai, Y., and Li, J. (2015). Core-shell structured SnO₂ hollow spheres-polyaniline composite as an anode for sodium-ion batteries. *RSC Adv.* 5, 31465–31471. doi: 10.1039/C5RA02834E
- Zheng, J., Tang, M., and Hu, Y. Y. (2016). Lithium ion pathway within Li₇La₃Zr₃O₁₂-polyethylene oxide composite electrolytes. *Angew. Chem. Int. Ed.* 55, 12538–12542. doi: 10.1002/anie.201607539
- Zhou, M., Xiong, Y., Cao, Y., Ai, X., and Yang, H. (2013). Electroactive organic anion-doped polypyrrole as a low cost and renewable cathode for sodium-ion batteries. *J. Polym. Sci. B.* 51:114. doi: 10.1002/polb.23184
- Zhou, M., Zhu, L. M., Cao, Y. L., Zhao, R. R., Qian, J. F., Ai, X. P., et al. (2012). Fe(CN)₆⁴⁻-doped polypyrrole: a high-capacity and high-rate cathode material for sodium-ion batteries. *RSC Adv.* 2, 5495–5498. doi: 10.1039/c2ra20666h
- Zhou, Q., Liu, L., Huang, Z., Yi, L., Wang, X., and Cao, G. (2016). Co₃S₄@polyaniline nanotubes as high-performance anode materials for sodium ion batteries. *J. Mater. Chem. A* 4, 5505–5516. doi: 10.1039/C6TA01497F
- Zhu, L. M., Shen, Y. F., Sun, M. Y., Qian, J. F., Cao, Y., Ai, X., et al. (2013). Self-doped polypyrrole with ionizable sodium sulfonate as a renewable cathode material for sodium ion batteries. *Chem. Commun.* 49, 11370–11372. doi: 10.1039/c3cc46642f
- Zia Ullah, K., Jesper, E., Mahiar Max, H., Roger, G., Hjalmar, G., Lars, W., et al. (2016). Thermoelectric polymers and their elastic aerogels. *Adv. Mater.* 28, 4556–4562. doi: 10.1002/adma.201505364

Conflict of Interest: The authors declare that the research was conducted in the absence of any commercial or financial relationships that could be construed as a potential conflict of interest.

Copyright © 2020 Romero, Mombrú, Pignanelli, Faccio and Mombrú. This is an open-access article distributed under the terms of the Creative Commons Attribution License (CC BY). The use, distribution or reproduction in other forums is permitted, provided the original author(s) and the copyright owner(s) are credited and that the original publication in this journal is cited, in accordance with accepted academic practice. No use, distribution or reproduction is permitted which does not comply with these terms.